The EMBO Journal vol.15 no.23 pp.6727–6738, 1996

Function of the *Evx-2* gene in the morphogenesis of vertebrate limbs

Yann Hérault, Suzanne Hraba-Renevey, Frank van der Hoeven and Denis Duboule[1]

Department of Zoology and Animal Biology, University of Geneva, Sciences III, Quai Ernest Ansermet 30, 1211 Geneva 4, Switzerland

[1]Corresponding author

Y.Hérault and S.Hraba-Renevey contributed equally to this work

Vertebrate gene members of the *HoxD* complex are essential for proper development of the appendicular skeletons. Inactivation of these genes induces severe alterations in the size and number of bony elements. *Evx-2*, a gene related to the *Drosophila even-skipped* (*eve*) gene, is located close to *Hoxd-13* and is expressed in limbs like the neighbouring *Hoxd* genes. To investigate whether this tight linkage reflects a functional similarity, we produced a null allele of *Evx-2*. Furthermore, and because *Hoxd-13* function is prevalent over that of nearby *Hoxd* genes, we generated two different double mutant loci wherein both *Evx-2* and *Hoxd-13* were inactivated *in cis*. The analysis of these various genetic configurations revealed the important function of *Evx-2* during the development of the autopod as well as its genetic interaction with *Hoxd-13*. These results show that, in limbs, *Evx-2* functions like a *Hoxd* gene. A potential evolutionary scenario is discussed, in which *Evx-2* was recruited by the *HoxD* complex in conjunction with the emergence of digits in an ancestral tetrapod.

Keywords: development/digits/*even-skipped*/gene targeting/genitalia

Introduction

Vertebrate limbs develop following a spatial–temporal progression so that proximal structures, such as those of the forearm, are determined before distal ones, such as digits (e.g. Tabin, 1995; Tickle, 1995). Proliferation is maximal in a distal area of the limb bud, the progress zone (PZ), wherein mesenchymal cells are under the influence of the overlaying epithelial cells; the apical ectodermal ridge (e.g. Cohn *et al.*, 1995; Parr and McMahon, 1995; Crossley *et al.*, 1996). Cells outside the PZ condense and generate the pre-chondrogenic cartilaginous blastemas. The resulting condensations will then undergo secondary modifications to form the definitive skeletal elements (Shubin and Alberch, 1986). Considerable evidence demonstrates that these morphogenetic processes require the function of those posterior *Hoxd* and *Hoxa* genes related to the *Drosophila Abdominal-B* homeotic gene (Izpisúa-Belmonte *et al.*, 1991). In tetrapods, *Hox* genes are clustered in four complexes, *HoxA*, *B*, *C* and *D*, localized on different chromosomes. Both their spatial expressions and temporal activations are co-linear with their positions along the chromosome such that genes located at the 3′ ends of the complexes are expressed earlier and in anterior domains, while 5′-located genes are expressed later and in progressively more posterior/distal areas (Dollé *et al.*, 1989; Gaunt *et al.*, 1989; Graham *et al.*, 1989). In developing limbs, gene inactivation experiments have shown that posterior *Hox* genes (from paralogous group 9 to 13) act in part by controlling local growth rates of the future skeletal elements (Dollé *et al.*, 1993; Small and Potter, 1993; Davis and Capecchi, 1994; Favier *et al.*, 1995; Fromental-Ramain *et al.*, 1996).

Evx-1 and *Evx-2*, two homeobox-containing cognates of the *Drosophila* pair-rule gene *even-skipped* (*eve*), are closely linked to the 5′ extremities of the *HoxA* and *HoxD* complexes, respectively (Bastian *et al.*, 1992). This linkage was observed in several vertebrate species (Bastian and Gruss, 1990; D'Esposito *et al.*, 1991; Faiella *et al.*, 1991; Bastian *et al.*, 1992; van der Hoeven *et al.*, 1996a) and probably reflects an ancestral configuration, for a comparable clustering was found in the coral *acropora* (Miles and Miller, 1992). Analysis of mouse *Evx-1* expression revealed an early activation during gastrulation and subsequent restriction to the posterior part of the embryo (Bastian and Gruss, 1990; Dush and Martin, 1992). These two features of *Evx-1* expression are shared by many genes belonging to the *even-skipped* family, in both vertebrates and invertebrates, and may therefore indicate an old functional trait of this gene family (see Dollé *et al.*, 1994). Accordingly, mice homozygous for an *Evx-1* gene disruption died at a pre-implantation stage (Spyropoulos and Capecchi, 1994). In contrast, the *Evx-2* gene is not expressed during early gastrulation. Instead, transcripts are detected only after the last *Hoxd* gene (*Hoxd-13*) has been activated, in the proctodeal area as well as in the limbs. This *Hox* type of regulation was postulated to result from a 'trapping effect', whereby *Evx-2* was activated in both limbs and genitalia by regulatory mechanisms acting on its neighbour gene *Hoxd-13*, as a result of the small distance which separates *Evx-2* from the *HoxD* complex (~8 kb; Dollé *et al.*, 1994). However, the question remained as to whether such a *Hox*-like expression of *Evx-2* merely reflected its neighbourhood with the *HoxD* complex or was accompanied by a true function during distal limb development.

We therefore inactivated the function of *Evx-2* by homologous recombination in embryonic stem (ES) cells. Because *Hoxd-13* was shown to be functionally prevalent over other *Hox* genes (Davis and Capecchi, 1996; Kondo *et al.*, 1996; van der Hoeven *et al.*, 1996b), two different double mutant alleles for *Evx-2* and *Hoxd-13* were also generated. Comparison between simple and double mutant mice demonstrated the non-additive aspect of the double

mutant phenotype. Mice lacking both *Evx-2* and *Hoxd-13* functions exhibited very severe alterations in the digital and carpal bony elements, thus showing the important role played by *Evx-2* during limb development even though its inactivation alone induced a mild phenotype confined to the autopod.

Results

Structure and comparative expression of Evx-2 and Hoxd-13

The mouse *Evx-2* gene was found ~8 kb upstream of the *Hoxd-13* gene (Figure 1A and B). While its intron–exon structure as well as its homeodomain sequence were rather different from that of a typical *Hoxd* gene, and though *Evx-2* was transcribed from the opposite DNA strand, the length of the *Evx-2–Hoxd-13* intergenic region was in the range of that observed between *Hoxd* genes belonging to the 9th to 13th groups of paralogy (Figure 1). Amino acid sequence comparison between the mouse *Evx-2* and *Hoxd-13* genes, on the one hand, and their zebrafish orthologous counterparts, on the other, revealed different levels of similarities. The complete sequence of the mouse *Evx-2* protein shared 78% identity with the zebrafish cognate (Figure 1E), whereas the *Hoxd-13* proteins were much more divergent (Figure 1F), with a fairly good homology in the homeodomain (78%, see also van der Hoeven *et al.*, 1996a), but an unusually low level of sequence identity in the first exon (<50%). Overall, the *Evx-2* sequence was thus much more conserved between vertebrate species than was that of *Hoxd-13*.

Whole-mount *in situ* hybridizations of *Evx-2* and *Hoxd-13* in 11.5 days post-coitum (d.p.c.) embryos illustrated the similarities in the expression patterns of both genes (Figure 2A). At this developmental stage, *Evx-2* transcripts were found restricted to the most distal parts of both the genital eminence (Figure 2A, arrow) and the presumptive digit areas of all four limb buds (Figure 2A, arrowheads). In addition, the onset of *Evx-2* expression, as shown for the hindlimbs, was localized to a posterior-distal part of the bud (Figure 2B, arrow). Subsequently, *Evx-2* expression extended to more distal and anterior parts to cover most of the future distal autopod (Figure 2A). In addition to the genital bud where *Evx-2* was expressed in the tip of the eminence (Figure 2C, arrow), a signal was found in the mesenchyme of the rectum (not shown) as well as in ventral cells just caudal to the genital eminence, probably within the tail gut (Figure 2C, arrowhead). Altogether, *Evx-2* was expressed throughout limb development in a manner very much reminiscent of the *Hoxd-13* expression pattern, except for a complex and dynamic expression in the central nervous system. This latter expression feature was, however, too weak to be detected clearly in our whole-mount *in situ* hybridizations (but see Dollé *et al.*, 1994).

Evx-2 loss of function

We investigated whether these similarities in expression patterns reflected common functional traits between *Evx-2* and *Hoxd-13*, by disrupting the *Evx-2* coding sequence through insertional mutagenesis via gene targeting (the $Evx\text{-}2^{Ge}$ allele; Figure 3). Progeny derived from heterozygous crosses showed the expected 1:2:1 Mendelian ratio in the segregation of genotypes. $Evx\text{-}2^{Ge/Ge}$ mutant mice were viable, although they displayed a 30% weight deficit at birth. This deficit was not compensated for at later developmental stages, even after several months. While homozygous females were normally fertile, $Evx\text{-}2^{Ge/Ge}$ males were not able to breed. As careful inspection of the male urogenital apparatus did not reveal any gross alteration, the cause of this sterility is unknown.

Limbs of adult mice homozygous for the $Evx\text{-}2^{Ge}$ allele showed highly penetrant, though rather weak, skeletal alterations. Firstly, and perhaps as a consequence of the growth deficit, $Evx\text{-}2^{Ge/Ge}$ limbs displayed a global decrease in size, mostly due to reduction in lengths of metacarpal and phalangeal bones, in all digits (Figure 4A and B). Moreover, bony elements in digit V (Figure 4A and B, brackets), as well as the d3 and d4 carpal bones were malformed (Figure 4C and D). For instance, while the second phalange (P2) of digit V was greatly reduced, the metacarpal was broader and abnormally enlarged, proximally (Figure 4B; brackets). In carpal bones of the distal row, changes were observed in the central (c), d3 and d4 bones. The central was longer than normal and extended below d2 and d3, while d3 pointed to the basis of metacarpal III (Figure 4D). In addition, d4 showed an abnormal indentation (Figure 4D, arrow). Comparison of younger wrists, at 4.5 days post-partum (d.p.p.), revealed that the cartilaginous condensation for d4 was split into several parts in the mutant wrist (Figure 4E and F). This alteration is likely to have derived from the early pre-chondrogenic pattern of cellular condensation, as the d4 carpal bone normally arises through the secondary fusion of two independent cartilaginous blastemas, as seen in fetal wrists (Figure 4G; d4 and d5). In mutant limbs, however, these two blastemas were not fused and a supernumerary condensation (d5*) appeared below the fifth metacarpal (Figure 4H). Eventually, d4 and d5 fused while d5* associated with the proximal part of metacarpal V (Figure 4F; d5*).

Double inactivation of Evx-2 and Hoxd-13

The inactivation of *Evx-2* generated a limb phenotype localized in domains where *Hoxd-13* is functional. Because the HOXD13 protein can suppress the function of other *Hoxd* genes (Davis and Capecchi, 1996; Kondo *et al.*, 1996; van der Hoeven *et al.*, 1996b), we assessed the function of *Evx-2* in the absence of *Hoxd-13* function, by producing two different lines of mice which carried mutations in both *Evx-2* and *Hoxd-13* in *cis*. The first line (Figure 5; EvD^{Ge1}) was produced by insertion of stop codons in the open reading frames (ORFs) of both *Evx-2* and *Hoxd-13*, using a restriction fragment extending from one gene to the other (Figure 5B, Stop*). A PGK*neo* selection cassette was introduced between the two genes, flanked by *loxP* sites to allow for its subsequent excision (Figure 5C and D). G418-resistant recombinant ES cell clones were obtained with different combinations of mutations, due to various recombination sites, and one clone was selected which had incorporated nonsense mutations in both genes (Figure 5C). For the second double mutant line (EvD^{Ge2}), the targeting construct used to generate the single *Evx-2* knock-out (the $Evx\text{-}2^{Ge}$ allele, Figures 3B and 6B) was electroporated into ES cells wherein *Hoxd-13* had already been inactivated by insertion of the *neomycin* gene (the $Hoxd\text{-}13^{St}$ allele; Figure 6A;

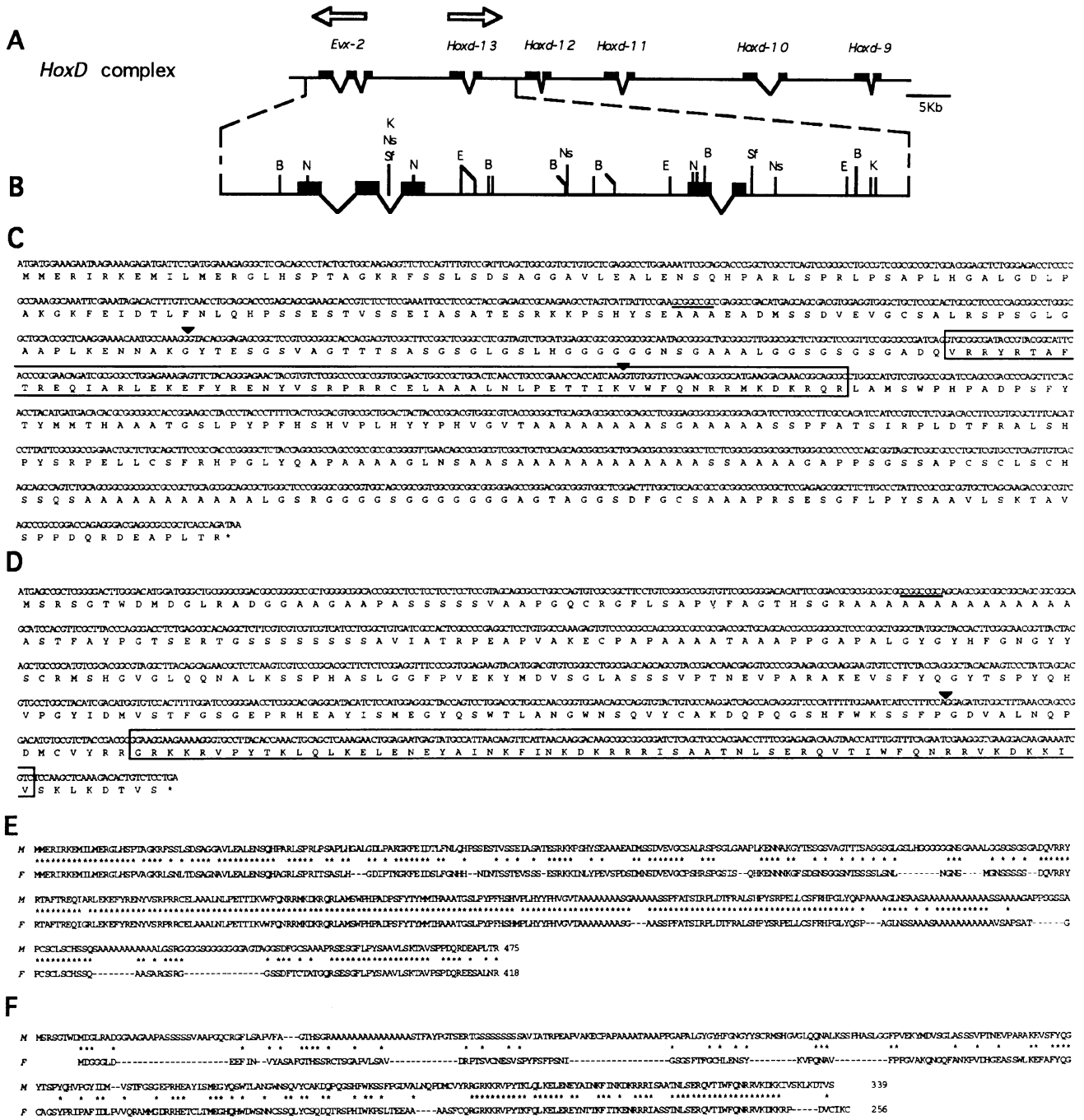

Fig. 1. Characterization of the murine *Evx-2* and *Hoxd-13* genes. (**A**) Map of the 5′ end of the *HoxD* complex. (**B**) Restriction map of the *Evx-2* and *Hoxd-13* intergenic region. Nucleotide and amino acid sequences of the murine *Evx-2* (**C**) and *Hoxd-13* genes (**D**). Homeoboxes are boxed. Positions of the introns are indicated by black arrowheads and the *Not*I sites used to introduce the stop codons in the two genes are underlined. Protein sequence comparison between mouse and zebrafish *Evx-2* (**E**) and *Hoxd-13* (**F**). The mouse (M) sequence is on the upper line. The asterisks indicate identical amino acid residues. B, *Bam*HI; N, *Not*I; Sf, *Sfi*I; K, *Kpn*I; E, *Eco*RI; Ns, *Nsi*I.

see also Dollé *et al.*, 1993). Restriction analysis indicated that both insertions were on the same chromosome (Figure 6D). Chimeric males were obtained and germline transmission was achieved for both targeting events.

Animals homozygous for the EvD^{Ge1} allele were viable but males were as yet unable to produce offspring. Mutant mice displayed a 30% weight deficit, probably due to the disruption of *Evx-2* (see above). In heterozygotes, skeletons appeared normal in all respects, whereas homozygous mice had rather strongly affected limbs, a phenotype clearly more pronounced than in the *Evx-2* simple mutant mice (Figure 7B, compare with Figure 4). In particular, the second phalanges (P2) of digits V and II were missing, and the metacarpal V was reduced and broader. Bony elements of digits II or III were fused and produced continuous, rigid bone rods (Figure 7B). Furthermore, an extra, non-segmented bone (VI) appeared post-axially with a high penetrance (80%). Many, if not all of the defects observed in distal carpal bones of $EvD^{Ge1/Ge1}$ mice were related to those seen with the

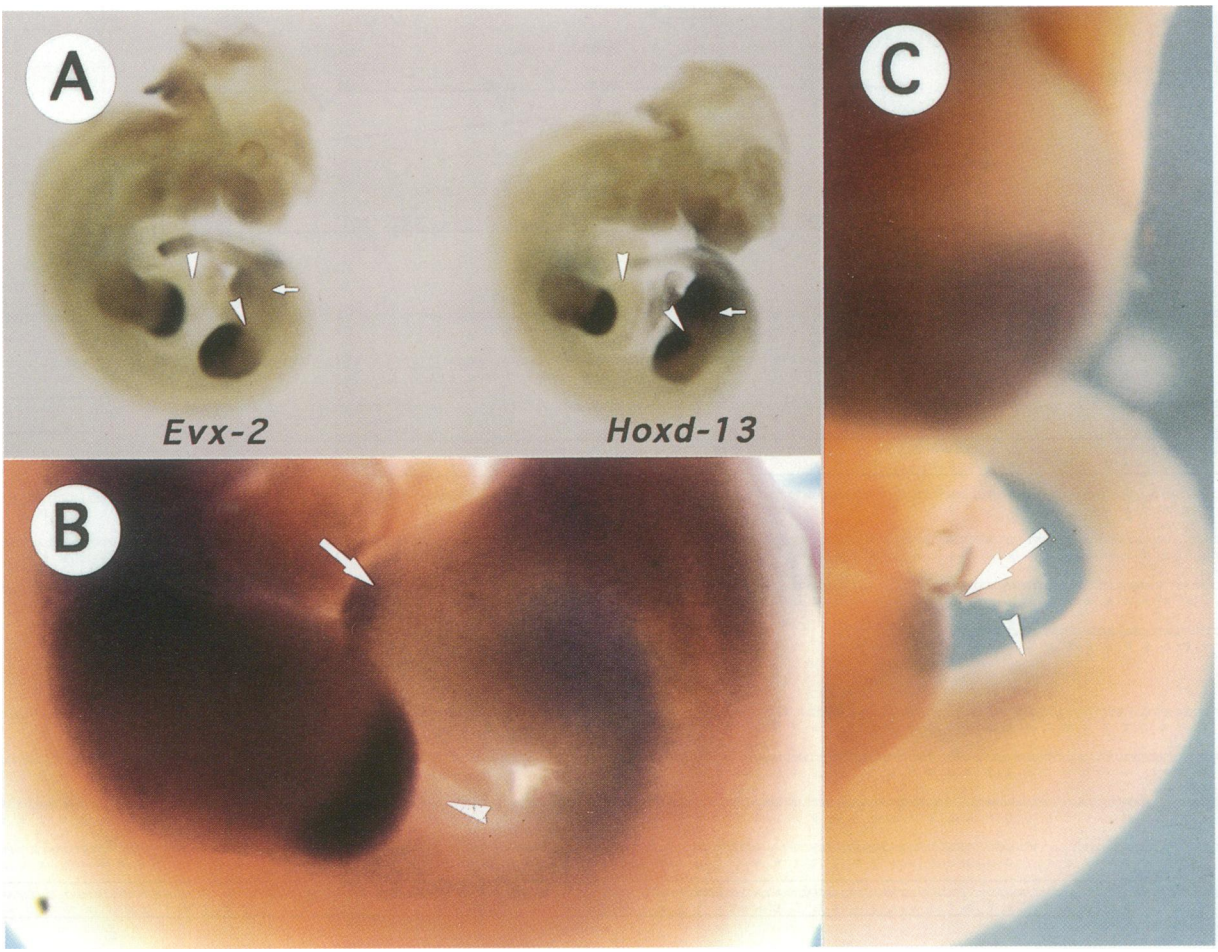

Fig. 2. Whole-mount *in situ* detection of *Evx-2* and *Hoxd-13* transcripts during mouse development. (**A**) Comparison of *Evx-2* and *Hoxd-13* expression in 11.5 d.p.c. mouse embryos. The domains are similar in both fore- and hindlimbs (white arrowhead) and in genitalia (white arrow). (**B**) At 10.5 d.p.c., *Evx-2* is expressed in distal parts of the forelimbs (white arrowhead), while its activation in the hindlimbs is confined to a distal and posterior area of the buds (white arrow). (**C**) Expression of *Evx-2* at 12.5 d.p.c. is restricted to the most distal part of the genital bud (white arrow) as well as to the ventral aspect of the tail, probably in the tail gut (white arrowhead).

Evx-2^{Ge} allele (Figure 8B and F; compare with Figure 4D and F). At 4.5 d.p.p., however, the split of the d4 bone was more pronounced in the wrist of *EvD*$^{Ge1/Ge1}$ animals (Figure 8F) than in those with the *Evx-2*$^{Ge/Ge}$ allele. This probably resulted from the removal of *Hoxd-13* function in the double mutant, for *Hoxd-13*$^{St/St}$ (null) animals often had a split d4 as well (Figure 8G; Dollé *et al.*, 1993). In adult *EvD*$^{Ge1/Ge1}$ mice, d4 remained as a single bone while the supernumerary d5 and d5* bones fused to the basis of metacarpal V (Figure 8B). In summary, the limb phenotype of *EvD*$^{Ge1/Ge1}$ was nearly identical to, though less severe than, that induced by the *Hoxd-13*St allele. However, the appearance of a novel phenotype associated with carpal bones suggested that *Evx-2* and *Hoxd-13* genetically interact with each other. This observation was confirmed by the analysis of the *EvD*^{Ge2} allele.

Mice heterozygous for the *EvD*^{Ge2} locus had normal looking limbs. While homozygous *EvD*$^{Ge2/Ge2}$ animals were obtained with a normal Mendelian ratio, half of them died during early post-natal development, probably as a result of their important weight deficit (up to 50%). Their limbs displayed severe alterations restricted to the autopods. All digits were markedly shortened, either due to a reduction and deformation of metacarpal and phalangeal bones, or to the absence of P2 in digits II and V (Figure 7D, arrows). Fusions occurred at most articulations, leading to single metacarpo-phalangeal elements. The thumb was altered as well and appeared as a single block with a hole at the level of the fusion between P1 and the metacarpus (Figure 7D, *). Moreover, *EvD*$^{Ge2/Ge2}$ mice had one additional element posteriorly and, often, a seventh digit emerged from post-axial rudimentary bones (Figure 7D). The wrist of *EvD*$^{Ge2/Ge2}$ mutant mice was similar to, though more severely affected than, that of *EvD*^{Ge1} homozygous animals, with a flattened central bone and abnormal d3 (Figure 8B and D). Alterations were also scored in the d4, d5 and d5* cartilage models (Figure 8H), where d4 always formed a small bone, whereas d5* either contacted the basis of an extra digit VI (Figure 8D) or fused with d5, as reported for the *EvD*^{Ge1} genotype (Figure 8B). In some cases, the aspect and position of d5* suggested a genuine articulation with the supernumerary digit (Figure 8D). Several small and ectopic bones appeared between the metacarpals and eventually fused either with the underlying carpal bones or with the metacarpus (Figure 8D; *).

Hindlimbs of mice carrying these different genetic configurations were affected in a similar way, and the

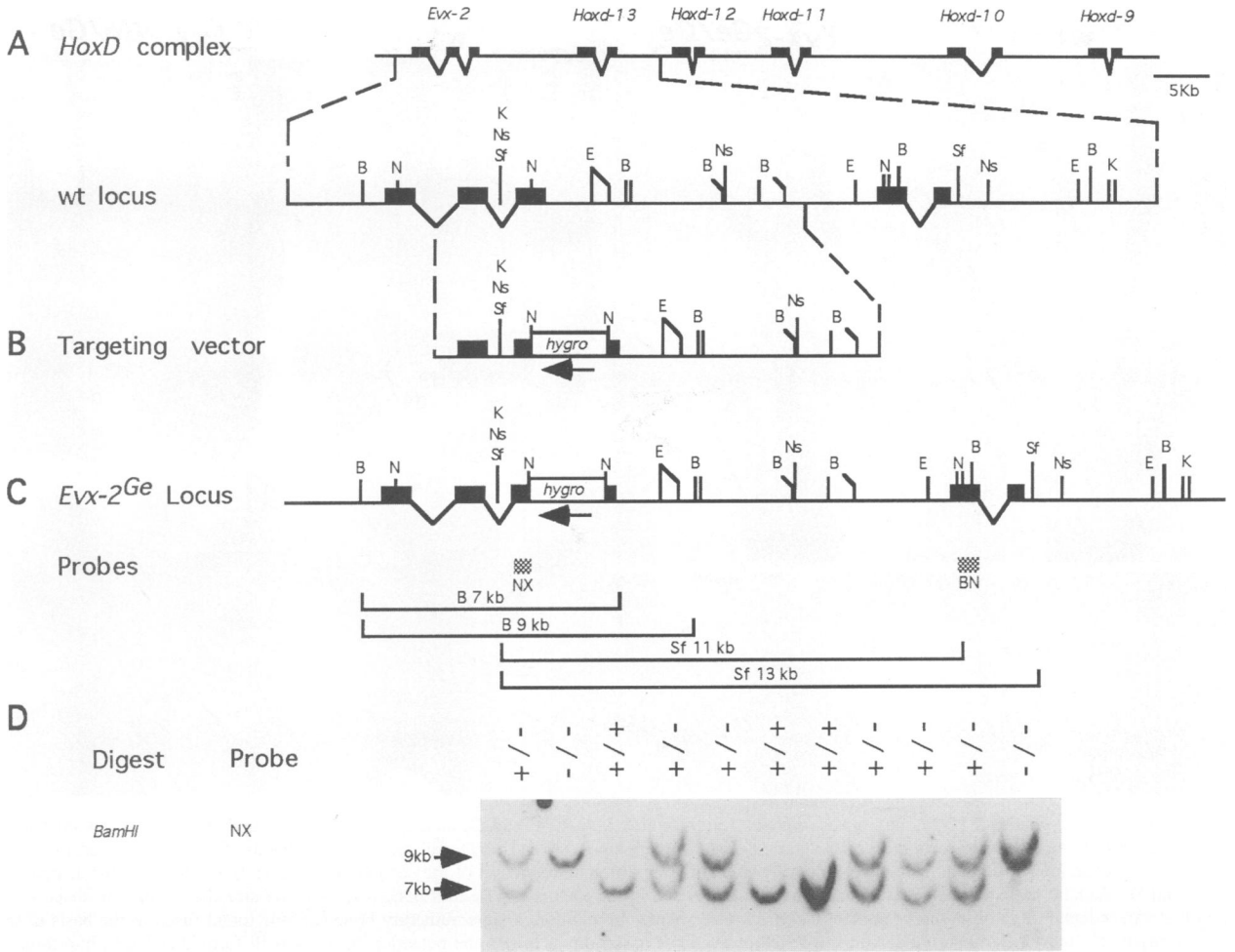

Fig. 3. The *Evx-2*^{Ge} allele. (**A**) Genomic structure of the 5′ part of the murine *HoxD* locus. (**B**) Targeting vector. (**C**) The *Evx-2*^{Ge} locus after homologous recombination. (**D**) Southern analysis of littermates produced by an *Evx-2*^{Ge} heterozygote cross. DNA was digested with *Bam*HI and hybridized with the NX probe to allow genotyping of the animals. The genotypes are indicated on the top with + for the wild-type allele and – for the recombined locus.

strength of each allele, as seen in the hands (see Figure 8), was reflected in the degree of hindlimb size reduction (Figure 9). The severity in reductions of bony elements followed a sequence which reflected the allelic series, so that only a moderate reduction was detected in metacarpus I of *Evx-2*$^{Ge/Ge}$ mice (Figure 9B), while a stronger effect was seen in *EvD*$^{Ge1/Ge1}$ animals (Figure 9C). Likewise, digits were altered more substantially in either *Hoxd-13*$^{St/St}$ (Figure 9D) or *EvD*$^{Ge2/Ge2}$ (Figure 9E) specimens, wherein digit I consisted of a single metacarpo-phalangeal element. Hence, in addition to the defects observed in the *Hoxd-13*$^{St/St}$ mutant hindlimbs, further defects in digits II and V were found in the double *Hoxd-13*/*Evx-2* (*EvD*^{Ge2}) homozygous feet, together with a sixth digit (Figure 9E) and supernumerary tarsal bones (Figure 9E, *).

To evaluate a potential effect of the PGK promoter in the recombined *EvD*^{Ge1} locus (Olson *et al.*, 1996), we excised the PGK*neo* selection cassette by crossing a mouse homozygous for *EvD*^{Ge1} with a Cre recombinase-expressing transgenic animal (Figure 5C and D, *EvD*^{Ge3}). Animals without the selection cassette were isolated and crossed to obtain homozygous mutants. The resulting phenotype was comparable with that shown by animals with the PGK*neo* cassette, with some alterations slightly reinforced such as the thickening and abnormal shape of metatarsal I (not shown). Novel phenotypic traits were not recovered, however, and the strengthening of some defects could result from the difference in genetic background introduced by the cross with the transgenic line. We thus considered that the presence of the PGK*neo* cassette, in this particular allele, did not affect the phenotype in an important way.

Discussion

Evx-2 is one of the murine genes orthologous to the *Drosophila* pair-rule gene *even-skipped* (*eve*). Unlike in Diptera, however, this vertebrate gene is linked closely to a *Hox* complex as it lies 8 kb upstream of the most 5′-located *Hoxd* gene, *Hoxd-13*. Interestingly, this close linkage is accompanied by a striking resemblance between the developmental expression patterns of *Evx-2* and the neighbouring *Hoxd* genes. In particular, *Evx-2* expression complies with temporal co-linearity, i.e. its onset of expression is not detected before that of *Hoxd-13* (Dollé *et al.*, 1994). Also, *Evx-2* is expressed strongly during limb development, in a distal domain which mimics that of posterior *Hoxd* genes such as *Hoxd-13*, *Hoxd-12* or

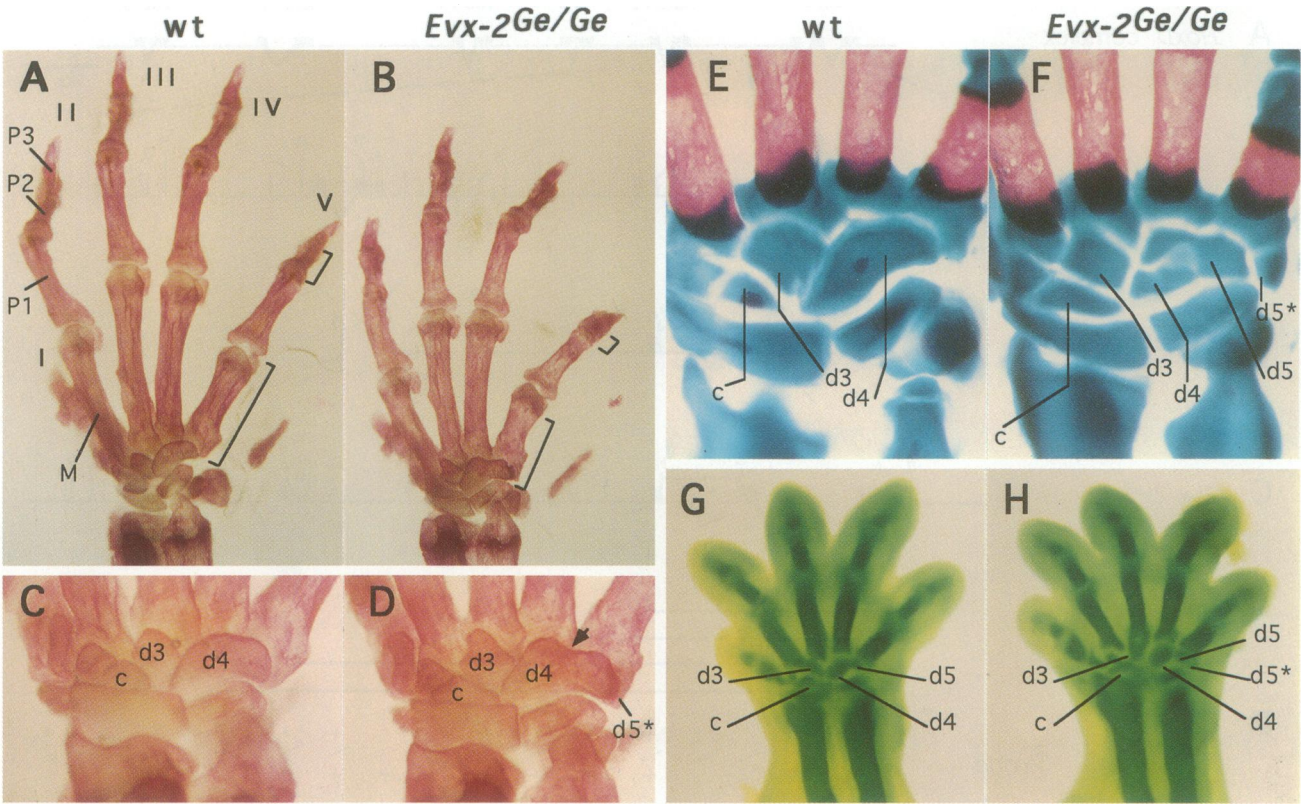

Fig. 4. Autopod defects in *Evx-2*$^{Ge/Ge}$ homozygous animals. Limbs from wt (A, C, E and G) or *Evx-2*$^{Ge/Ge}$ (B, D, F and H) homozygous littermates are compared after bone (A–D) or cartilage (E–H) stainings, at different stages. (**A** and **B**) Dorsal view of adult hands stained with alizarin red. Note the overall size reduction of the hand in mutant animals and the disproportionate reduction of the second phalange (P2) and the fifth metacarpal bone (M). (**C** and **D**) Skeletal preparations of wt (C) and mutant (D) wrists. In the mutant, the central bone (c) is slightly stretched while the shape of d3 is modified. An indentation is observed on mutant d4 (black arrowhead). In addition, a supernumerary bone (d5*) is found fused to the basis of the fifth metacarpus. (**E** and **F**) Cartilage models in the developing carpus at 4.5 d.p.p. In (F), the posterior-distal d4 is ill formed and split into three bones (d4, d5 and d5*), while the shapes of c and d3 are slightly, but reproducibly, abnormal. (**G** and **H**) Chondrogenic pattern in 14.5 d.p.c. fetal hands. Three separate blastemas are detected in the posterior-distal region of the mutant forelimb (H, d4, d5 and d5*), while only two are found in wt hands. I–V, digit numbers, from anterior (thumb) to posterior (minimus); M, metacarpal bones; P1–P3, phalanges; d1–d4, carpal bones of the distal row.

Hoxd-11. Recently, gene transposition experiments have shown that expression in this distal limb domain, the presumptive digit area, was dependent on the position of a given gene in the complex, rather than upon a gene-specific regulatory control, such that genes introduced between *Evx-2* and *Hoxd-13* became expressed in digits (van der Hoeven *et al.*, 1996b). In this context, we asked whether *Evx-2* expression in the future digits reflected a genuine function, potentially responsible for the maintainance of the linkage of this gene to the *HoxD* complex or, alternatively, if this expression merely resulted from this linkage without a specific function in developing distal appendages. To discriminate between these possibilities, we inactivated *Evx-2* by gene targeting, either alone or in combination with *Hoxd-13*. We produced two different double knock-out alleles *in cis*, which allowed us to conclude that *Evx-2* has an important function during the morphogenesis of the autopods.

Inactivation of Evx-2

Animals homozygous for the inactivation of *Evx-2* displayed a severe weight deficit and males were unable to breed. The reason for the deficit in weight is unclear, but is probably linked to the role of *Evx-2* in the central nervous system where it is expressed late during development. This deficit was of 30%, on average, while a 10% deficit was observed for *Hoxd-13* mutant animals (Dollé *et al.*, 1993). As far as the hypofertility is concerned, *Evx-2* mutant animals were similar to *Hoxd-13*$^{St/St}$ males, although *Hoxd-13* mutants bred on rare occasions. These two genes are expressed in the genital bud and uro-genital sinus (Dollé *et al.*, 1994) and their disruptions might, therefore, affect some accessory glands involved in reproduction, or certain mechanical aspects linked to breeding behaviour. Alterations of the ano-rectal region and uro-genital system have been reported previously after inactivations of posterior *Hox* gene (Dollé *et al.*, 1993; Hsieh-Li *et al.*, 1995; Rijli *et al.*, 1995; Satokata *et al.*, 1995; Kondo *et al.*, 1996), and similar alterations may result from removing *Evx-2* function.

Upon skeletal preparation, a subtle but visible phenotype was found in the distal carpal region as well as in digit V. These phenotypic traits, stronger in forelimbs than in hindlimbs, were similar to those reported for other 5′-located *Hox* genes and involved related bony elements of the distal limbs (Dollé *et al.*, 1993; Small and Potter, 1993; Davis and Capecchi, 1994; Davis *et al.*, 1995; Favier *et al.*, 1995, 1996; Kondo *et al.*, 1996). However, as for the case of *Hoxd-11* and *Hoxd-12*, but in contrast to *Hoxd-13*, only a minor part of the expression domain

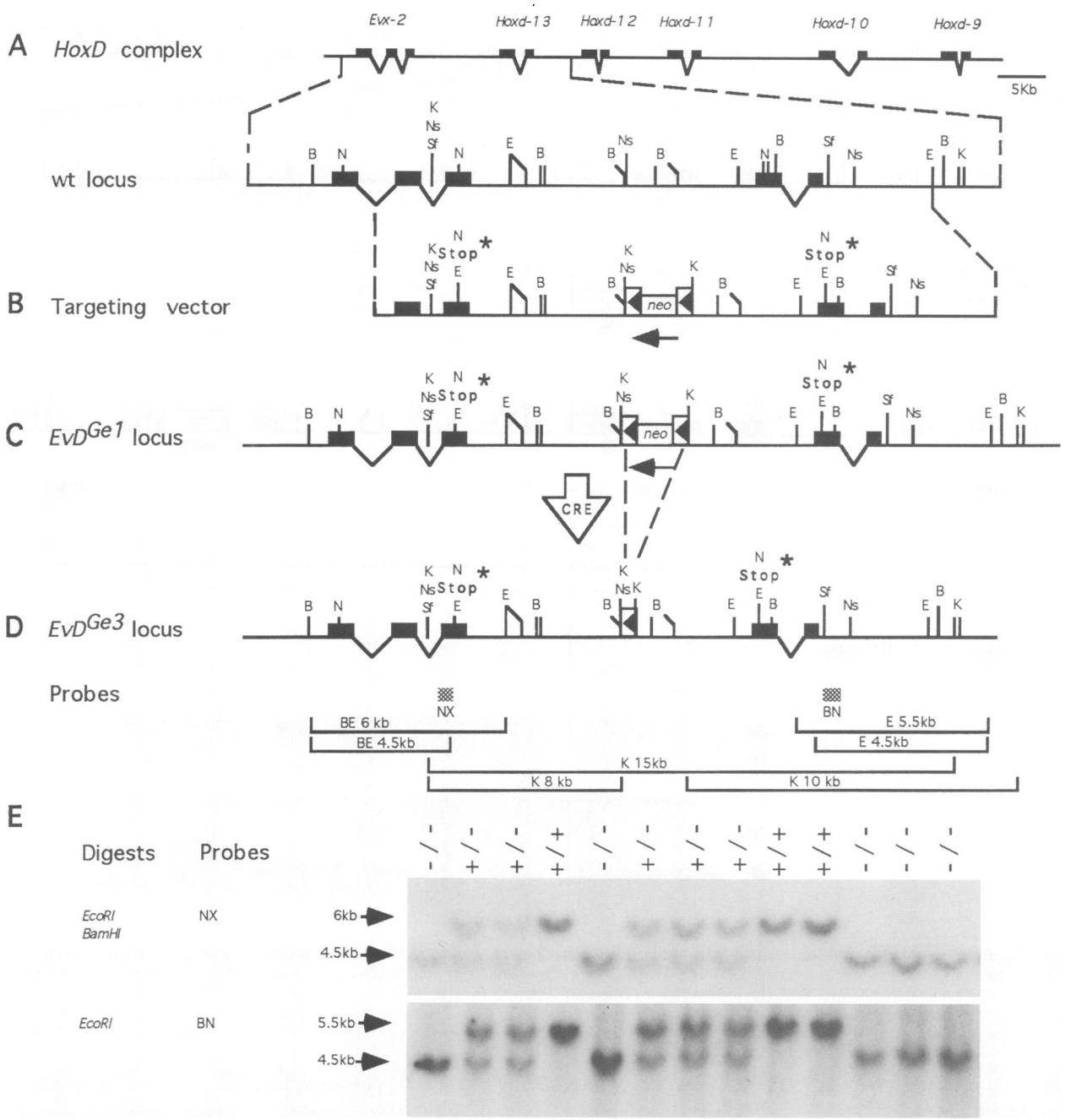

Fig. 5. The EvD^{Ge1} double mutant locus. (**A**) 5′ part of the *HoxD* complex. (**B**) Targeting vector with stop codons in the two frames (Stop*) and the PGK*neo* selection cassette in between the two genes. (**C**) The EvD^{Ge1} mutant locus after recombination. (**D**) Treatment of EvD^{Ge1} mice with Cre recombinase excised the selection cassette to generate the EvD^{Ge3} locus. (**E**) Genotyping of littermates resulting from an EvD^{Ge1} heterozygote cross. DNA was digested either with *Eco*RI and *Bam*HI, or with *Eco*RI alone, and hybridized to either the NX or the BN probes (indicated in D), to determine the genotype of the animals (indicated on the top of the blots).

was affected, suggesting that the function of *Evx-2* could be compensated for, or masked by other proteins.

Evx-2 and Hoxd-13 inactivations in cis

Two different alleles were obtained for the double inactivation of *Hoxd-13* and *Evx-2*. EvD^{Ge1} was generated by interrupting both *Evx-2* and *Hoxd-13* ORFs in the first exons, while EvD^{Ge2} was produced by targeting the *Evx-2* gene in the $Hoxd\text{-}13^{St}$ chromosome (Dollé *et al.*, 1993). Heterozygous animals of either genotype were indistinguishable from their control littermates. However, homozygotes showed severe alterations in the autopods (see below). Interestingly, important differences in the strength of the phenotypes were observed between the two configurations, with the double insertional mutant (EvD^{Ge2}) being much stronger than the double nonsense mutations (EvD^{Ge1}). A comparison between phenotypic traits of EvD^{Ge1} and $Hoxd\text{-}13^{St/St}$ animals suggested that the former animals did not entirely lack *Hoxd-13* function. Such a *Hoxd-13* hypomorph allele could derive from protein reinitiation downstream of the stop codon which may rescue part of the phenotype. Although an *in vitro* translation assay for the efficiency of the mutation did not produce any detectable protein (not shown), we cannot rule out

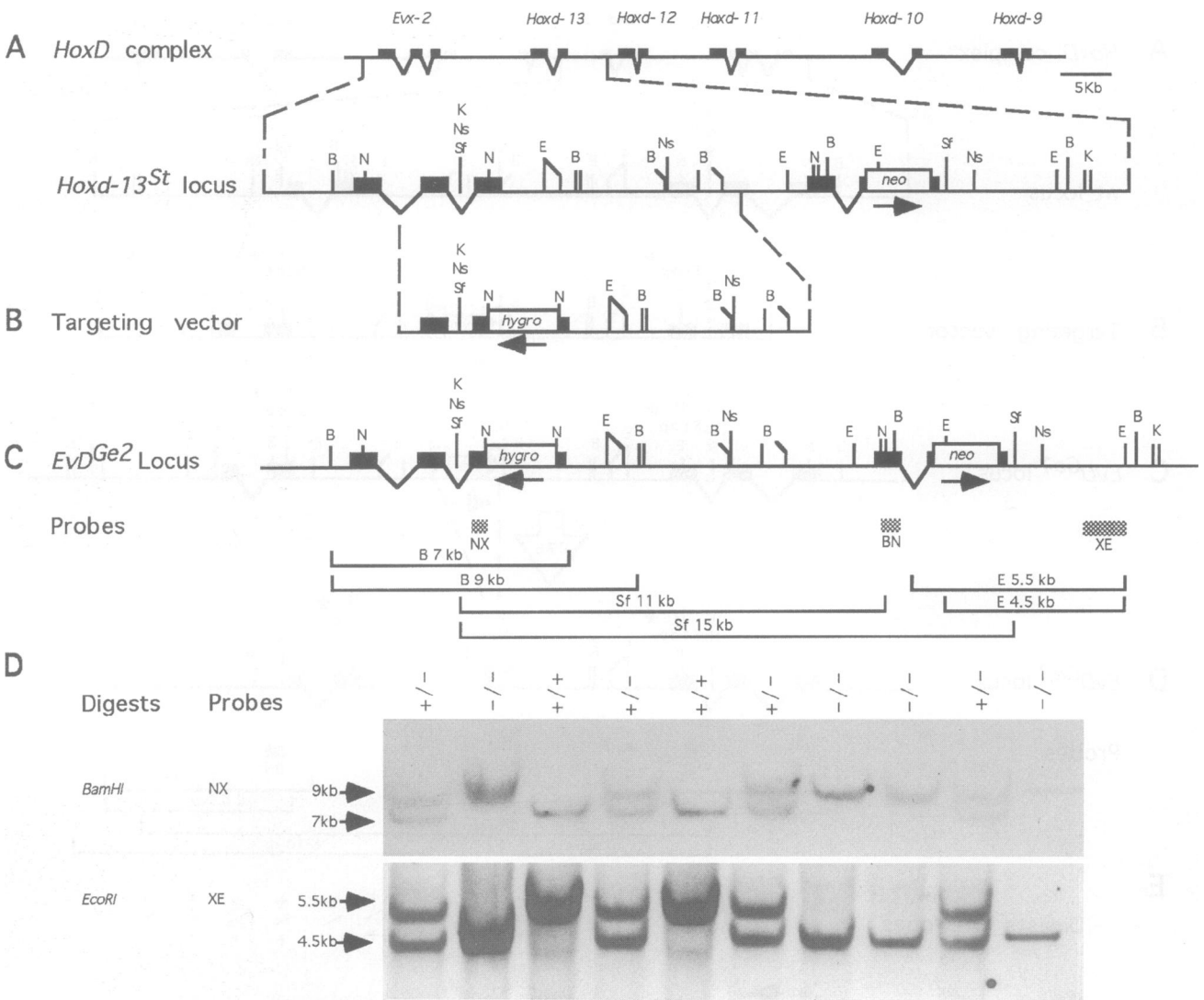

Fig. 6. The EvD^{Ge2} double mutant locus. (**A**) 5′ part of the *HoxD* complex with, below, a chromosome already targeted at the *Hoxd-13* locus. (**B**) *Evx-2* targeting vector (same as in Figure 3B). (**C**) The EvD^{Ge2} mutant locus after homologous recombination. Both genes are inactivated by insertions of different selectable markers. (**D**) Genotyping of littermates derived from an EvD^{Ge2} heterozygote cross. DNA was digested with either *Bam*HI or *Eco*RI, and hybridized to either the NX or the XE probes (shown in C) to determine the genotype of the animals (on top of the blots).

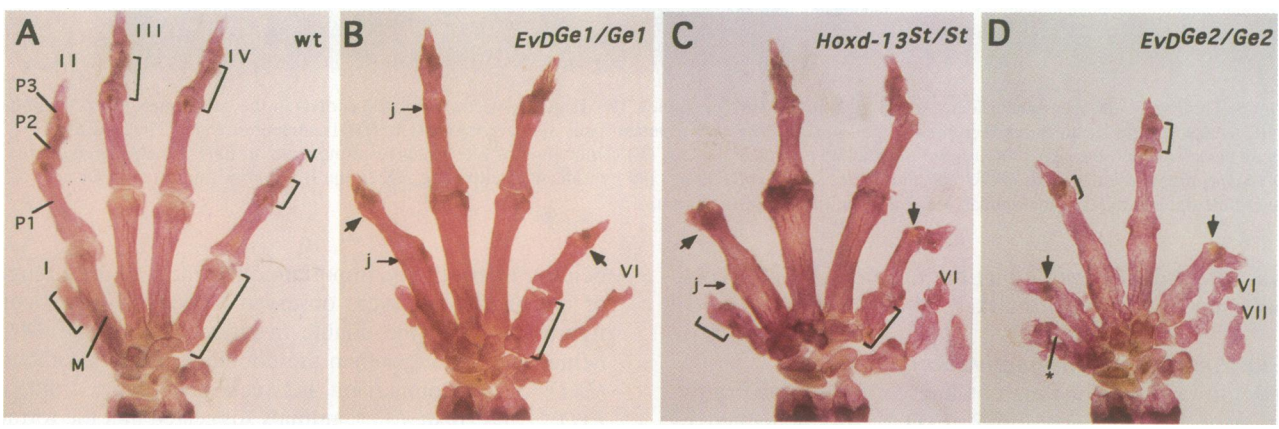

Fig. 7. Alterations in the hands of adult mutant animals. A wt control hand (**A**) is compared with mutant hands from either EvD^{Ge1} (**B**), $Hoxd\text{-}13^{St}$ (**C**) or EvD^{Ge2} (**D**) homozygous animals. Note the gradation in size reduction of the hands (from left to right) and the accompanying increasing severity in the alterations of digits, strikingly exemplified by the size reduction of the fifth metacarpal bone MV (bracket), the presence or absence of P2s (black arrows) or the fusions (j) at the metacarpo-phalangeal joint as well as between phalanges, which were much more severe in the case of the $EvD^{Ge2/Ge2}$ locus (D). Furthermore, in this latter animal, the thumb was reduced, ill formed and partly split (D,*). I–V, digit number from thumb to minimus; VI and VII in (B), (C) and (D) indicated extended nodules or true post-axial digits made out of rudimentary bones. M, metacarpal; P1–P3, phalanges.

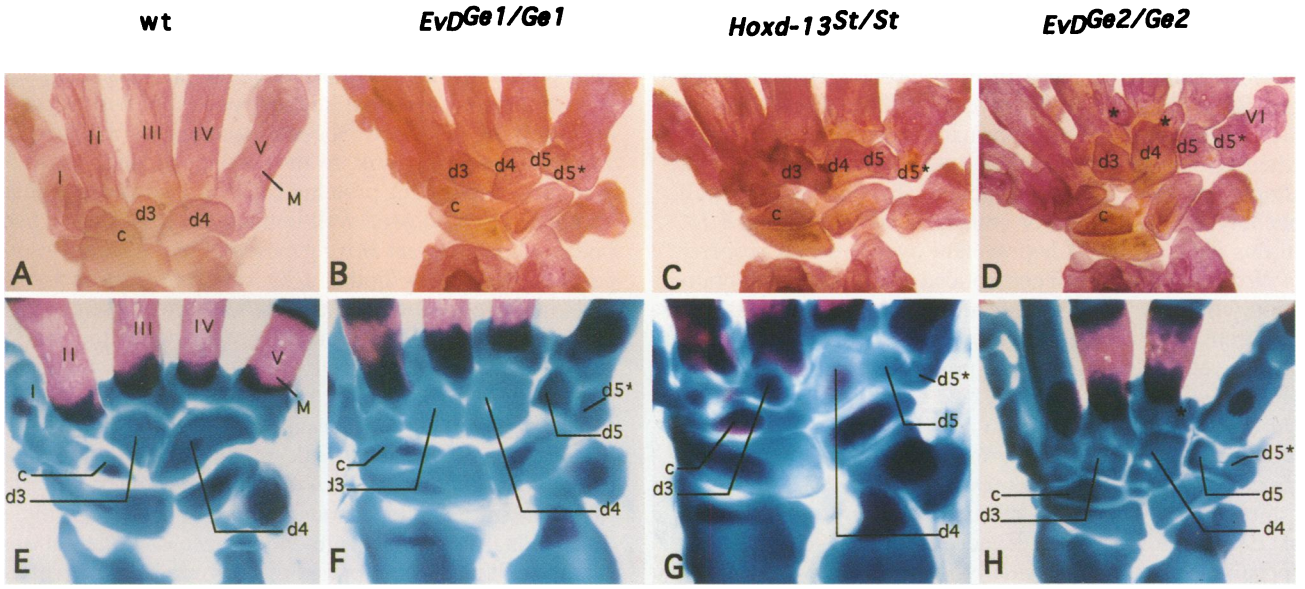

Fig. 8. Skeletal defects in the wrists of homozygous mutant animals. Wt carpus (**A** and **E**) are shown together with that of EvD^{Ge1} (**B** and **F**), $Hoxd\text{-}13^{St}$ (**C** and **G**) and EvD^{Ge2} (**D** and **H**) mutant mice. Panels on the top are adult preparations while those at the bottom are from 4.5 d.p.p. animals. Malformations of the centrale (c) and d3 carpal bones in $EvD^{Ge1/Ge1}$ (B) and $EvD^{Ge2/Ge2}$ (D) animals are related to the phenotype displayed by $Evx\text{-}2^{Ge}$ homozygote mutants. d4 was more affected in double mutants (B and D) than in the $Hoxd\text{-}13^{St/St}$ animals (C). This was due to the abnormal fusions of d5 with the extra d5* blastemas. While both models fused to the basis of metacarpal of V in $EvD^{Ge1/Ge1}$ (B and F), only d5* did so in $Hoxd\text{-}13^{St/St}$. In $EvD^{Ge2/Ge2}$ animals, however, d5 and d5* were either fused together (H) or d5* became involved in the articulation of an additional digit VI (VI in H). In this latter case, numerous supernumerary small bones appeared scattered in the wrist but preferentially in the distal row, at the bases of the metas (*).

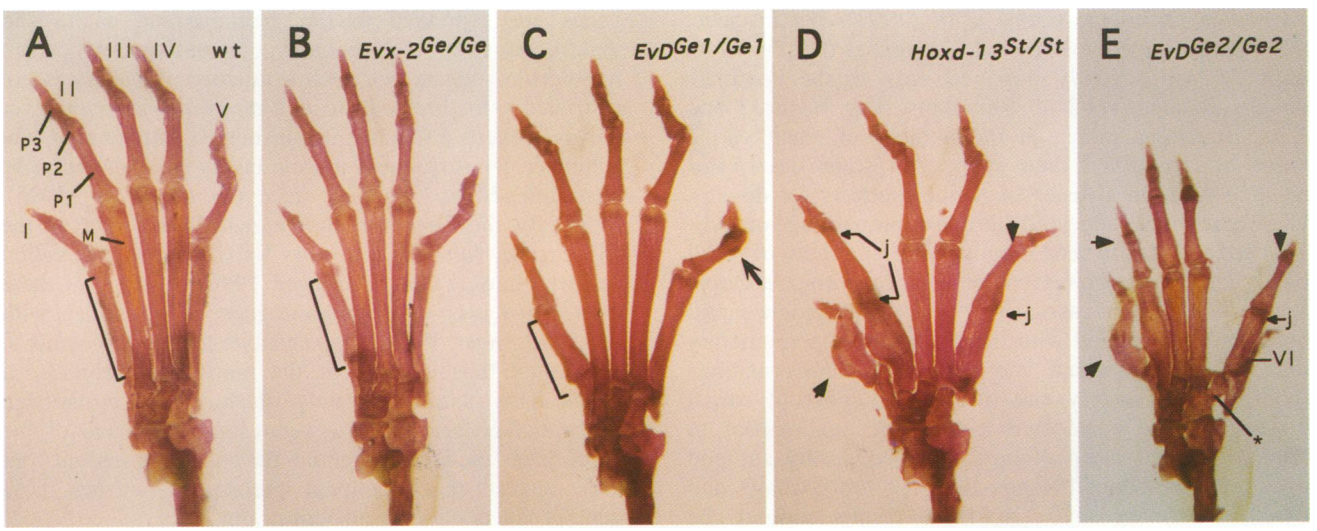

Fig. 9. Hindlimb phenotypes of adult mice of the various genetic constitutions. (**A**) wt control foot; (**B**) $Evx\text{-}2^{Ge}$; (**C**) EvD^{Ge1}; (**D**) $Hoxd\text{-}13^{St}$; (**E**) EvD^{Ge2}. Note the progressive reduction in the size of the foot and the increasing severity of the phenotype (from left to right). While the metatarsal I started to be slightly reduced in length in both $Evx\text{-}2^{Ge/Ge}$ (B) and $EvD^{Ge1/Ge1}$ (C) animals (brackets), the entire digit I appeared as a single curved element in either $Hoxd\text{-}13^{St/St}$ or $EvD^{Ge2/Ge2}$ mice (black arrowhead in D and E). This alteration was also observed in the EvD^{Ge3} homozygous mice (not shown). P1 of digit V, normal in $Evx\text{-}2^{Ge}$, was altered in the EvD^{Ge1} allele (C, black arrow) as well as in the double mutant feet, where it was fused to MV. The P2 of digit II, which was present but fused to P1, in the $Hoxd\text{-}13^{St/St}$ mutant (j in D), was absent from the EvD^{Ge2} foot (arrow in E), as well as from digit V (arrows in D and E). (*; VI) indicate the supernumerary tarsal bone and digit, respectively, in (E).

the possibility that a small quantity of truncated HOXD13 protein was produced *in vivo*. Alternatively, a weak *Hoxd-13* function could be achieved by an as yet undetected alternatively spliced mRNA species, initiating upstream and spliced to the homeobox. There was no sign of such a functional rescue with the *Evx-2* nonsense mutation, as all the alterations found in the simple *Evx-2* mutant animals, in particular the carpal bone defect, were also recovered in the double EvD^{Ge1} mutant animals. From this, we concluded that the EvD^{Ge1} configuration led to an *Evx-2* null mutation combined, *in cis*, with a hypomorph *Hoxd-13* allele. In contrast, the EvD^{Ge2} animals lacked both functions. Variations in strengths of phenotypes after using different strategies to inactivate a *Hox* gene have been reported in another case (Ramirez-Solis *et al.*, 1993).

Hoxd-like function of Evx-2 in the autopod

The phenotypes described in this study demonstrate both the involvement of *Evx-2* in limb morphogenesis and its genetic interaction with *Hoxd-13*. While *Evx-2* mutant digits appeared essentially normal, the alterations produced when removing both functions were very severe and not simply additive. Therefore, most of the simple *Evx-2* null phenotype was hidden, or compensated for, by *Hoxd-13*. In this view, *Hoxd-13* is prevalent over *Evx-2*, a property of *Hoxd-13* which had been noticed already upon combination with other posterior *Hoxd* mutant alleles (Davis and Capecchi, 1996; Kondo *et al.*, 1996). Consequently, we cannot yet totally rule out the possibility that the function of the *Evx-2* product, in wild-type digits, is suppressed by *Hoxd-13*. In the absence of a *Hoxd-13* product, an *Evx-2* function may be uncovered, raising the possibility that the *Hoxd-13* mutant phenotype (Dollé *et al.*, 1993; Davis and Capecchi, 1996) may be rescued partly by other HOXD or EVX2 proteins (see Kondo *et al.*, 1996) and thus appears weaker than it actually is.

The various combinations of *Evx-2* and *Hoxd-13* alleles led to a gradation in the severity of the phenotypes. Clearly, the addition of disrupted alleles generated increasingly reduced autopods, truncated digits and scattered small bones in the carpus. Interestingly, the sequence in which bony elements were affected, upon removing successive doses of the two genes, was the reverse of their sequence of appearance during limb ontogeny (Shubin and Alberch, 1986), corroborating previous observations on the *Hoxd-13* mutant phenotype (Dollé *et al.*, 1993). For instance, the weakest phenotype ($Evx\text{-}2^{Ge}$) involved digit V, while digit IV was severely impaired only in the complete double mutant $EvD\text{-}2^{Ge2}$. Removing both *Hoxd-13* and *Evx-2* functions increased the number of small carpal bones and modified their shapes. In some cases, this resulted from an absence of fusion (such as for d4–d5), while other bones appeared due to ectopic cartilage models. This led to a malformed carpus, with an excess of small bones in a way reminiscent of a more primitive carpal structure. In several cases, a posterior-distal ectopic carpal bone even articulated with the basis of a supernumerary digit. These important morphological transformations (both the polydactyly and increased number of carpal bones) may be considered as atavisms and appear to reflect ancestral morphologies observed during autopod evolution (see Hinchliffe and Johnson, 1980; Coates and Clack, 1990). In any case, these results support the proposal that modifications in the expression of these genes could have been linked to important transformations during the evolution of limb morphologies (e.g. Dollé *et al.*, 1993).

The molecular and cellular mechanisms by which *Evx-2* and *Hoxd* genes exert their functions are unknown. However, the results described here and elsewhere (e.g. Dollé *et al.*, 1993; Morgan and Tabin, 1994; Davis *et al.*, 1995; Davis and Capecchi, 1996) help to define a few emerging tendencies. First, it seems that the genes themselves have poorly individualized functions. The absolute number of gene doses, i.e. the quantity of information, seems to be dominant over its quality (e.g. Davis *et al.*, 1995), even though some proteins may be functionally stronger than others, such as HOXD13. In molecular terms, this may reflect a poor discrimination for target binding sites, even between proteins harbouring rather different homeodomain sequences (such as, for example, *Evx-2* versus *Hoxd-13*). One possibility is that most of these proteins recognize the same set of target binding sequences but with variable affinities. In this view, the construction of a particular morphology may result from a subtle balance between amounts of different proteins rather than from a precise combination (code) of well-defined gene products. Secondly, while different *Hoxd* genes are functional in various parts of developing limbs, a constant observation is that their inactivation leads to cell deficit (Dollé *et al.*, 1993; Davis *et al.*, 1995; Davis and Capecchi, 1996; this work). It is reasonable, therefore, to envisage an involvement of these genes in the control of either cell proliferation or cell recruitment for condensation (Dollé *et al.*, 1993). In this view, HOX proteins could modulate the proliferation of cellular subpopulations within the limb buds, in order to transform a homogeneous cellular space into a three-dimensional network of pre-chondrogenic condensations. Likewise, it has been reported that *Hox* genes are involved in the control of cellular aggregation capacities (Yokouchi *et al.*, 1995). Changes in cell adhesive properties may modify cell recruitment during chondrogenesis leading, for example, to phalangeal fusions or to the appearance of post-axial polydactyly. Within this conceptual framework, *Evx-2* appeared to behave like any posterior *Hoxd* genes.

We report here that the similarities in the expression domains of *Hoxd-13* and *Evx-2*, during limb development, are paralleled by functional analogies. The facts that both genes are expressed in the genitalia and analia and that males from both homozygous null genotypes are hypofertile suggest that such a functional analogy is not restricted to the limbs. Instead, it may take place wherever *Hoxd-13* exerts a function, for instance in the internal anal sphincter, whose smooth muscle layers were shown to be altered in *Hoxd-13* mutant mice (Kondo *et al.*, 1996). Strikingly, the *Caenorhabditis elegans* counterpart of the *Evx-2* gene, *vab-7*, is necessary for the proper generation of rectal muscle cells (Ahringer, 1996). In some of these cells, *vab-7* is co-expressed and genetically interacts with *egl-5* (Ahringer, 1996), the nematode gene orthologous to *AbdB* and thus cognate of the murine posterior *Hoxd* genes. This parallel not only illustrates the remarkable functional conservation between some members of the *HOX* gene family throughout the animal kingdom, but also suggests that functional interactions between these gene products have an ancient origin.

An ancestral linkage between Evx-2 and Hoxd-13?

The observation that *eve*-related genes are found linked to a *HOX* complex in vertebrates (Bastian *et al.*, 1992; van der Hoeven *et al.*, 1996a) and corals (Miles and Miller, 1992) suggests that this genomic configuration reflects an ancestral organization (Dollé *et al.*, 1994). In nematodes, the distance between *vab-7* and the *HOX* complex is large, in the range of 1–2 Mb (Ahringer, 1996), indicating that, as for *Drosophila*, there is no strict functional requirement to maintain a close genomic linkage. An ancestral localization of *Evx* at the 'posterior' end of the complex was probably associated with an important function in the posterior part of the developing animal, as illustrated by the vertebrate *Evx-1* or *eve-1* genes (Joly *et al.*, 1993; Spyropoulos and Capecchi,

1994) or by *vab-7* (Ahringer, 1996). After large-scale duplications of the *HOX* complexes, which occurred during chordate phylogeny (Garcia-Fernandez and Holland, 1994), *Evx-2* was probably brought into the close vicinity (8 kb) of the *HoxD* complex and, consequently, became dependent upon regulatory controls acting on this complex. This is reflected by the *Hoxd*-like expression in distal limbs and genitalia, as well as by the suppression of the early-posterior expression, conceivably due to the repressive effect of the *HoxD* complex (temporal co-linearity; see van der Hoeven *et al.*, 1996b). Unlike *Evx-2*, *Evx-1* remained at some distance (~ 50 kb), preventing a similar control from the *HoxA* complex from occurring (Dollé *et al.*, 1994). This latter gene thus conserved a crucial function during gastrulation (Spyropoulos and Capecchi, 1994) while *Evx-2* was recruited for digit development. This newly acquired, *Hoxd*-like function of *Evx-2* may have represented a substantial functional help for *Hoxd* genes, thus explaining this close linkage in more evolved vertebrates. The genomic analysis of the posterior *HoxD* complex in a variety of animals species will be interesting in this respect.

Materials and methods

Cloning, sequencing and whole-mount in situ hybridizations

Both *Evx-2* and *Hoxd-13* were cloned during our walk on the *HoxD* complex (Dollé *et al.*, 1991; Bastian *et al.*, 1992; van der Hoeven *et al.*, 1996a). Sequences of reading frames were established and can be found in the EMBL database under the accession Nos X87752, X99290 and X99291. The *Hoxd-13* and *Evx-2* probes were as described previously (Dollé *et al.*, 1994) and were labelled with digoxigenin-11-UTP (Boehringer). Embryos were fixed overnight in 4% paraformaldehyde and whole-mount *in situ* hybridization was performed according to established procedures. Staining was done using an alkaline phosphatase-conjugated anti-digoxigenin antibody.

Targeting vectors and ES cell lines

DNA fragments containing the *Evx-2* and the *Hoxd-13* genes were cloned from a 129/SV genomic DNA library (Dollé *et al.*, 1991; Izpisúa-Belmonte *et al.*, 1991). The *Evx-2*^{Ge} targeting vector was produced by inserting the PGK*hygro* selectable cassette into a *Not*I site in the first exon of the murine *Evx-2* gene. As a consequence, the *Evx-2* coding sequence was interrupted after the 110th amino acid residue. The targeting vector was linearized and electroporated, either into wild-type D3 ES cells (Doetschman *et al.*, 1985), for the single knock-out experiment (*Evx-2*^{Ge}), or into the *Hoxd-13*$^{+/St}$ D3-derived cell line (Dollé *et al.*, 1993), for the double *Evx-2/Hoxd-13* knock-out (*EvD*^{Ge2}). Maintenance and electroporation of ES cells were according to standard procedure (Joyner, 1993), and resistant cells were selected with hygromycin at 150 μg/ml for 10 days. A single *Evx-2*^{Ge} clone was recovered (out of 200 selected colonies) which had recombined at the expected locus. The integrity of both the 3′ and 5′ parts of the targeted locus were examined with the NX and BN probes, respectively, which gave either a 9 kb *Bam*HI fragment (targeted locus) instead of a 7 kb (wt locus), or a 13 kb instead of an 11 kb *Sfi*I fragment. The same strategy was used to identify homologous recombinants leading to the production of the *EvD*^{Ge2} locus. Additional probes were used to verify these various recombinations (not shown). The targeting vector *EvD*^{Ge1} was designed to introduce stop codons in both *Evx-2* and *Hoxd-13* ORFs, so that translation of the *Evx-2* and *Hoxd-13* mRNAs would end after the 110th and 58th amino acid residue, respectively (see Figure 1). Furthermore, a 153 bp deletion was induced into the *Hoxd-13* gene by removing a *Not*I fragment. Termination codons were inserted by using a linker oligonucleotide which introduced novel *Eco*RI sites used to detect the mutations. Oligonucleotide insertions were controlled further by DNA sequencing. The PGK*neo* gene was introduced into a unique *Nsi*I site located in the middle of the *Evx-2/Hoxd-13* intergenic region. A *Kpn*I genomic digest probed with the BN and NX probes (see Figure 5) was used to detect homologous recombination. The introduction of the two stop mutations was verified using, for *Evx-2*, a 3.5 kb *Eco*RI–*Bam*HI fragment detected with the NX probe and, for *Hoxd-13*, a 4.5 kb *Eco*RI fragment detected with the BN probe. Other probes confirmed that recombination occurred correctly.

Mutant lines and skeletal analysis

Chimaeras were obtained by microinjection of ES cells into C57Bl/6j blastocysts (Joyner, 1993). Germline transmission was monitored by Southern blot analysis. Individual breeding colonies were established for the *Evx-2*^{Ge}, *EvD*^{Ge1} and *EvD*^{Ge2} mutants. The *Hoxd-13*St mutation has been described previously (Dollé *et al.*, 1993). The PGK*neo* cassette was removed from the *EvD*^{Ge1} chromosome by crossing homozygous mice with a mouse expressing the Cre recombinase under the control of the cytomegalovirus (CMV) promoter (gift of P.Chambon and J.Brocard) giving rise to *EvD*^{Ge3}. All mice were derived from C57Bl6×Sv129 crosses, except for *EvD*^{Ge3} which was mixed with the transgenic background (see text). For skeletal analysis, mice were collected, processed and stained with alizarin red, for bones, and/or alcian blue for cartilage material, according to established procedures (Inouye, 1976).

Acknowledgements

We would like to thank Drs R.Kemler, A.Smith, P.Kastner, K.Rajewski, P.Chambon and J.Brocard for kindly providing us with the D3 ES cells, the LIF expression vector, a *loxP*-PGK*neo*-*loxP* cassette, the Cre recombinase expression vector and a Cre recombinase expressing mouse, respectively. We thank M.Friedli and N.Fraudeau for their invaluable help with cell cultures and genomic typing and Drs J.Zákány and T.Kondo for helpful discussions and suggestions on the manuscript. Y.H. was the recipient of fellowships from the EMBO and ARC and S.H.-R. from the Marie Heim-Vögtlin foundation. This work was supported by funds from the Swiss National Research Fund, the Canton de Genève, the Claraz Foundation, the Latsis Foundation and the HFSPO.

References

Ahringer,J. (1996) Posterior patterning by the *Caenorhabditis elegans even-skipped* homolog *vab-7*. *Genes Dev.*, **10**, 1120–1130.

Bastian,H. and Gruss,P. (1990) A murine even-skipped homologue, *Evx 1*, is expressed during early embryogenesis and neurogenesis in a biphasic manner. *EMBO J.*, **9**, 1839–1852.

Bastian,H., Gruss,P., Duboule,D. and Izpisúa-Belmonte,J.C. (1992) The murine even-skipped-like gene *Evx-2* is closely linked to the *Hox-4* complex, but is transcribed in the opposite direction. *Mamm. Genome*, **3**, 241–243.

Coates,M.I. and Clack,J.A. (1990) Polydactyly in the earliest known tetrapod limbs. *Nature*, **347**, 66–69.

Cohn,M.J., Izpisúa-Belmonte,J.C., Abud,H., Heath,J.K. and Tickle,C. (1995) Fibroblast growth factors induce additional limb development from the flank of chick embryos. *Cell*, **80**, 739–746.

Crossley,P.H., Minowarda,G., MacArthur,C.A. and Martin,G.R. (1996) Roles for *FGF8* in the induction, initiation and maintenance of chick limb development. *Cell*, **84**, 127–136.

Davis,A.P. and Capecchi,M.R. (1994) Axial homeosis and appendicular skeleton defects in mice with a targeted disruption of *Hoxd-11*. *Development*, **120**, 2187–2198.

Davis,A.P. and Capecchi,M.R. (1996) A mutational analysis of the 5′ *HoxD* genes: dissection of genetic interactions during limb development in the mouse. *Development*, **122**, 1175–1185.

Davis,A.P., Witte,D.P., Hsieh-Li,H.M., Potter,S.S. and Capecchi,M.R. (1995) Absence of radius and ulna in mice lacking *Hoxa-11* and *Hoxd-11*. *Nature*, **375**, 791–795.

D'Esposito,M., Morelli,F., Acampora,D., Migliaccio,E., Simeone,A. and Boncinelli,E. (1991) *EVX2*, a human homeobox gene homologous to the even-skipped segmentation gene, is localized at the 5′ end of *HOX4* locus on chromosome 2. *Genomics*, **10**, 43–50.

Doetschman,T.C., Eistetter,H., Katz,M., Schmidt,W. and Kemler,R. (1985) The *in vitro* development of blastocyst-derived embryonic stem cell lines: formation of visceral yolk sac, blood islands and myocardium. *J. Embryol. Exp. Morphol.*, **87**, 27–45.

Dollé,P., Izpisúa-Belmonte,J.C., Falkenstein,H., Renucci,A. and Duboule,D. (1989) Coordinate expression of the murine *Hox-5* complex homeobox-containing genes during limb pattern formation. *Nature*, **342**, 767–772.

Dollé,P., Izpisúa-Belmonte,J.C., Boncinelli,E. and Duboule,D. (1991) The *Hox-4.8* gene is localized at the 5′ extremity of the Hox-4 complex and is expressed in the most posterior parts of the body during development. *Mech. Dev.*, **36**, 3–13.

Dollé,P., Dierich,A., LeMeur,M., Schimmang,T., Schuhbaur,B., Chambon,P. and Duboule,D. (1993) Disruption of the *Hoxd-13* gene induces localized heterochrony leading to mice with neotenic limbs. *Cell*, **75**, 431–441.

Dollé,P., Fraulob,V. and Duboule,D. (1994) Developmental expression of the mouse *Evx-2* gene: relationship with the evolution of the *HOM/Hox* complex. *Development*, Suppl., 143–153.

Dush,M.K. and Martin,G.R. (1992) Analysis of mouse *Evx* genes: *Evx-1* displays graded expression in the primitive streak. *Dev. Biol.*, **151**, 273–287.

Faiella,A. *et al.* (1991) Isolation and mapping of *EVX1*, a human homeobox gene homologous to *even-skipped*, localized at the 5′ end of *HOX1* locus on chromosome 7. *Nucleic Acids Res.*, **19**, 6541–6545.

Favier,B., Le Meur,M., Chambon,P. and Dollé,P. (1995) Axial skeleton homeosis and forelimb malformations in Hoxd-11 mutant mice. *Proc. Natl Acad. Sci. USA*, **92**, 310–314.

Favier,B., Rijli,F.M., Fromental-Ramain,C., Fraulob,V., Chambon,P. and Dollé,P. (1996) Functional cooperation between the non-paralogous genes *Hoxa-10* and *Hoxd-11* in the developing forelimb and axial skeleton. *Development*, **122**, 449–460.

Fromental-Ramain,C., Warot,X., Lakkaraju,S., Favier,B., Haack,H., Birling,C., Dierich,A., Dollé,P. and Chambon,P. (1996) Specific and redundant functions of the paralogous *Hoxa-9* and *Hoxd-9* genes in forelimb and axial skeleton patterning. *Development*, **122**, 461–472.

Garcia-Fernandez,J. and Holland,P.W. (1994) Archetypal organization of the amphioxus *Hox* gene cluster. *Nature*, **370**, 563–566.

Gaunt,S.J., Krumlauf,R. and Duboule,D. (1989) Mouse homeo-genes within a subfamily, *Hox-1.4*, *-2.6* and *-5.1*, display similar anteroposterior domains of expression in the embryo, but show stage- and tissue-dependent differences in their regulation. *Development*, **107**, 131–141.

Graham,A., Papalopulu,N. and Krumlauf,R. (1989) The murine and *Drosophila* homeobox gene complexes have common features of organization and expression. *Cell*, **57**, 367–378.

Hinchliffe,J.R. and Johnson,D.R. (1980) *The Development of the Vertebrate Limb. An Approach Through Experiment, Genetics, and Evolution*. Oxford Science Publications, Clarendon Press, Oxford.

Hsieh-Li,H.M., Witte,D.P., Weinstein,M., Branford,W., Li,H., Small,K. and Potter,S.S. (1995) *Hoxa 11* structure, extensive antisense transcription, and function in male and female fertility. *Development*, **121**, 1373–1385.

Inouye,M. (1976) Differential staining of cartilage and bone in fetal mouse skeleton by alcyan blue and alizarin red. *S. Cong. Anom.*, **16**, 171–173.

Izpisúa-Belmonte,J.C., Falkenstein,H., Dollé,P., Renucci,A. and Duboule,D. (1991) Murine genes related to the *Drosophila AbdB* homeotic genes are sequentially expressed during development of the posterior part of the body. *EMBO J.*, **10**, 2279–2289.

Joly,J.S., Joly,C., Schulte-Merker,S., Boulekbache,H. and Condamine,H. (1993) The ventral and posterior expression of the zebrafish homeobox gene *eve1* is perturbed in dorsalized and mutant embryos. *Development*, **119**, 1261–1275.

Joyner,A.L. (1993) *Gene Targeting: A Practical Approach*. Oxford University Press Inc., New York.

Kondo,T., Dollé,P., Zákány,J. and Duboule,D. (1996) Function of posterior *HoxD* genes in the morphogenesis of the anal sphincter. *Development*, **122**, 2651–2659.

Miles,A. and Miller,D.J. (1992) Genomes of diploblastic organisms contain homeoboxes: sequence of *eveC*, an even-skipped homologue from the cnidarian *Acropora formosa*. *Proc. R. Soc. Lond.*, **248**, 159–161.

Morgan,B.A. and Tabin,C. (1994) *Hox* genes and growth: early and late roles in limb bud morphogenesis. *Development*, Suppl., 181–186.

Olson,E.N., Arnold,H.-H., Rigby,P.W.J. and Wold,B.J. (1996) Know your neighbors: three phenotypes in null mutants of the myogenic bHLH gene *MRF4*. *Cell*, **85**, 1–4.

Parr,B.A. and McMahon,A.P. (1995) Dorsalizing signal *Wnt-7a* required for normal polarity of D-V and A-P axes of mouse limb. *Nature*, **374**, 350–353.

Ramirez-Solis,R., Zheng,H., Whiting,J., Krumlauf,R. and Bradley,A. (1993) *Hoxb-4* (*Hox-2.6*) mutant mice show homeotic transformation of a cervical vertebra and defects in the closure of the sternal rudiments. *Cell*, **73**, 279–294.

Rijli,F.M., Matyas,R., Pellegrini,M., Dierich,A., Gruss,P., Dollé,P. and Chambon,P. (1995) Cryptorchidism and homeotic transformations of spinal nerves and vertebrae in *Hoxa-10* mutant mice. *Proc. Natl Acad. Sci. USA*, **92**, 8185–8189.

Satokata,I., Benson,G. and Maas,R. (1995) Sexually dimorphic sterility phenotypes in *Hoxa10*-deficient mice. *Nature*, **374**, 460–463.

Shubin,N.H. and Alberch,P. (1986) A morphogenetic approach to the origin and basic organization of the tetrapod limb. *Evol. Biol.*, **20**, 319–387.

Small,K.M. and Potter,S.S. (1993) Homeotic transformation and limb defects in *Hoxa-11* mutant mice. *Genes Dev.*, **7**, 2318–2382.

Spyropoulos,D.D. and Capecchi,M.R. (1994) Targeted disruption of the *even-skipped* gene, *evx1*, causes early postimplantation lethality of the mouse conceptus. *Genes Dev.*, **8**, 1949–1961.

Tabin,C. (1995) The initiation of the limb bud: growth factors, Hox genes, and retinoids. *Cell*, **80**, 671–674.

Tickle,C. (1995) Vertebrate limb development. *Curr. Opin. Genet. Dev.*, **5**, 478–484.

van der Hoeven,F., Sordino,P., Fraudeau,N., Izpisúa-Belmonte,J.C. and Duboule,D. (1996a) Teleost *HoxD* and *HoxA* genes: comparison with tetrapods and functional evolution of the HOXD complex. *Mech. Dev.*, **54**, 9–21.

van der Hoeven,F., Zákány,J. and Duboule,D. (1996b) Gene transpositions in the *HoxD* complex reveal a hierarchy of regulatory controls. *Cell*, **85**, 1025–1035.

Yokouchi,Y., Nakazato,S., Yamamoto,M., Goto,Y., Kameda,T., Iba,H. and Kuroiwa,A. (1995) Misexpression of Hoxa-13 induces cartilage homeotic transformation and changes cell adhesiveness in chick limb buds. *Genes Dev.*, **9**, 2509–2522.

Received on July 18, 1996; revised on August 22, 1996